

Explosive Synchronization is Discontinuous

Vladimir Vlasov¹, Yong Zou², and Tiago Pereira³

Institute of Physics, Potsdam University, Germany

Department of Physics, East China Normal University, Shanghai, 200062, China

Department of Mathematics, Imperial College London, London SW72AZ, UK

September 20, 2018

Abstract

Spontaneous explosive is an abrupt transition to collective behavior taking place in heterogeneous networks when the frequencies of the nodes are positively correlated to the node degree. This explosive transition was conjectured to be discontinuous. Indeed, numerical investigations reveal a hysteresis behavior associated with the transition. Here, we analyze explosive synchronization in star graphs. We show that in the thermodynamic limit the transition to (and out) collective behavior is indeed discontinuous. The discontinuous nature of the transition is related to the nonlinear behavior of the order parameter, which in the thermodynamic limit exhibits multiple fixed points. Moreover, we unravel the hysteresis behavior in terms of the graph parameters. Our numerical results show that finite size graphs are well described by our predictions.

1 Introduction

Many networks in nature exhibit a heterogeneous behavior in the node's degrees, with some nodes being massively connected whereas the remaining nodes are sparsely connected [1]. These heterogeneous networks exhibit intricate collective properties [2, 3, 4]. Of particular interest is a situation where on top of each node we have an oscillator whose (isolated) frequency positively correlates with the node's degree. In such a setting, as one increases the interaction strength among nodes an abrupt transition towards collective behavior is observed [5]. This abrupt transition to collective behavior, called explosive synchronization, appears not to be model specific and has been observed in electronic circuits [6], time delayed systems [7], and a second order Kuramoto model [8].

Two distinct features of explosive synchronization have attracted a great deal of attention. First, its abrupt character leading to an apparently discontinuous transition [5, 6, 7, 8, 9, 10, 11, 12, 13, 14]. Second, the hysteresis behavior associated with the two distinct transitions: forward and backward transitions. The forward transition is characterized by a fast transition from an incoherent state to a coherent one as the interaction strength increases. Whereas in the backward transition one starts at a stable coherent state and as the coupling strength decreases a sudden transition to

an incoherent state takes place. The critical coupling for the forward transition does not coincide with that of the backward transition. Moreover, there is evidence that such a hysteretic loop is determined by the network's structural parameters [15].

To uncover the nature of the transition, one needs to understand the global behavior of the order parameter. However, this requires one to globally solve the equations of motion, which is impractical for a general network. Recently, using star graphs as motifs and a series of approximations it was possible to study the transition and thereby to reinforce the abrupt character of the transition [13, 14, 15, 16]. However, the dynamical behavior of the order parameters and the precise nature of the transition remain undisclosed.

We investigate the explosive transition of Kuramoto oscillators in a star graph, which consists of a central hub connected to N nodes. Here, we show that in the thermodynamics limit, when the system size goes to infinity, the model is fully solvable. We obtain two fundamental results:

1. Transitions associated with explosive synchronization are discontinuous.
2. There is a hysteresis loop associated with explosive synchronization.

We obtain these results by employing the Watabe-Strogatz (WS) approach [17, 18, 19], which yields an exact nonlinear equation for the order parameter. The stability analysis reveals the existence of parameter regions where the order parameter exhibits multi-stability. These coexisting fixed points lead to the hysteresis behavior and to both forward and backward discontinuous transitions. The main mechanism generating the forward discontinuity is the following

The asynchronous dynamics corresponds to a fixed point of the order parameter. After reaching a critical coupling value the fixed point disappears and the only remaining fixed point corresponds to the synchronized state.

We also check our predictions against finite size effects. Our numerics reveal that the finite size fluctuations are negligible. Since, star graphs are fundamental building blocks for intricate structures such as scale-free networks, our findings can be used as paradigms to unravel the transition.

2 The Model

Let us consider the star network of N leaf nodes and a central hub described by

$$\dot{\varphi}_k = \omega + \lambda \sin(\psi - \varphi_k) \quad \text{for } k = 1, 2, \dots, N \quad (1)$$

$$\dot{\psi} = \beta\omega + \beta \frac{\lambda}{N} \sum_{k=1}^N \sin(\varphi_k - \psi) \quad (2)$$

where we have normalized the frequency of the leaves to unit and $\beta > 1$ corresponding to the positive correlation between the degree and frequency. Here, we introduce a slight modification to Refs. [5, 15], which concerns the rescaled coupling strength for the hubs. The reason is that we will consider the thermodynamic limit $N \rightarrow \infty$, so the normalization is necessary to make sense of the limit. In practice, this normalization is immaterial as one only considers finite size effects.

3 Fully Solvable Limit: Nonlinear evolution law for the order parameter

Our goal is to employ the WS change of coordinates and solve the model fully. The model is fully solvable because all nodes have the same frequency (isolated). To perform the analysis, we first introduce the phase difference

$$\theta_k = \varphi_k - \psi. \quad (3)$$

Next, we rewrite the equations for θ_k in the setting of WS approach

$$\dot{\theta}_k = -(\beta - 1)\omega - \beta\lambda\text{Im}(G(t)) + \lambda\text{Im}(e^{-i\theta_k}), \quad (4)$$

$$G(t) = \frac{1}{N} \sum_{j=1}^N e^{i\theta_j}, \quad (5)$$

and the equation for ψ remains unchanged. Now we applied the WS approach for Eq. (4) [17, 18]. We make use of the WS variable transform in the form presented in [19], that is,

$$e^{i\varphi_k} = \frac{z + e^{i(\xi_k + \alpha)}}{1 + z^* e^{i(\xi_k + \alpha)}}, \quad (6)$$

where $z = z(t)$, $\alpha = \alpha(t)$ are global variables and ξ_k are constants that depend on the initial conditions of the system (4) (for more details see [19]). Next, we need to express $G(t)$ in terms of new variables. In the general case, the expression for $G(t)$ is rather complex, but in the thermodynamic limit $N \rightarrow \infty$ and uniform distribution of constants ξ_k

$$\sigma(\xi) = (2\pi)^{-1},$$

where σ denotes the density. In this variables, we obtain

$$G(t) = z,$$

where z is a complex number and $|z|$ is the order parameter. The WS approach yields a closed system of equations for the global macroscopic variables

$$\dot{z} = i[-(\beta - 1)\omega - \beta\lambda\text{Im}(z)]z + \lambda \frac{1 - z^2}{2}, \quad (7)$$

$$\dot{\alpha} = -(\beta - 1)\omega - \beta\lambda\text{Im}(z) + \lambda\text{Im}(z^*). \quad (8)$$

Since α does not enter in the equation for z , so we can consider the equation for z separately.

3.1 Fixed Points for the Order parameter

The fixed points of the first equation in (7) are

$$z_{s1,2} = \exp \left\{ i \arcsin \left(-\frac{(\beta-1)\omega}{(\beta+1)\lambda} \right) \right\}, \quad \text{if } \lambda > \lambda_c^f, \quad (9)$$

$$z_{a1,2} = -i \frac{(\beta-1)\omega \pm \sqrt{(\beta-1)^2\omega^2 - (2\beta+1)\lambda^2}}{(2\beta+1)\lambda}, \quad \text{and} \quad (10)$$

$$z_{s1,2} = \exp \left\{ i \arcsin \left(-\frac{(\beta-1)\omega}{(\beta+1)\lambda} \right) \right\}, \quad \text{if } \lambda_c^f \geq \lambda \geq \lambda_c^b, \quad (11)$$

$$z_{a2} = -i \frac{(\beta-1)\omega - \sqrt{(\beta-1)^2\omega^2 - (2\beta+1)\lambda^2}}{(2\beta+1)\lambda}, \quad \text{if } \lambda < \lambda_c^b. \quad (12)$$

where λ_c^f and λ_c^b corresponds to the forward and backward critical couplings

$$\lambda_c^f = \frac{\beta-1}{\sqrt{2\beta+1}}\omega \quad \text{and} \quad \lambda_c^b = \frac{\beta-1}{\beta+1}\omega$$

In order to study the stability of the fixed points (9) we linearize the system around the corresponding fixed point. First, for two asynchronous fixed points $z_{a1,2}$ we obtain the following linearized system:

$$\begin{aligned} \dot{a} &= \mp \left((\beta+1) \sqrt{\lambda_c^b - \frac{2\beta+1}{(\beta+1)^2} \lambda^2} \right) b, \\ \dot{b} &= - \left(\frac{\beta(\beta+1)}{2\beta+1} \lambda_c^b \mp \frac{(\beta+1)^2}{2\beta+1} \sqrt{\lambda_c^b - \frac{2\beta+1}{(\beta+1)^2} \lambda^2} \right) a, \end{aligned}$$

where $a = \text{Re}(z)$ and $b = \text{Im}(z) - \text{Im}(z_{a1,2})$ respectively. From (13) it follows that the fixed point with “+” z_{a1} is a saddle for $\lambda > \lambda_c^b$ and the fixed point with “-” z_{a2} is neutrally stable center (for more detail see [20]). Second, for two synchronous fixed points z_{s1} (with positive real value) and z_{s2} (with negative real value):

$$\begin{aligned} \dot{a} &= \mp \left(\sqrt{\lambda^2 - (\lambda_c^b)^2} \right) a - \lambda_c^b b, \\ \dot{b} &= \mp \left((\beta+1) \sqrt{\lambda^2 - (\lambda_c^b)^2} \right) b, \end{aligned}$$

where $a = \text{Re}(z) - \text{Re}(z_{s1,2})$ and $b = \text{Im}(z) - \text{Im}(z_{s1,2})$ respectively. From (13) it follows that for $\lambda > \lambda_c^b$ the fixed point with positive real value z_{s1} is sink (stable) node and the fixed point with negative real value z_{s2} is source (unstable) node. The fixed points (9) are shown on (Fig. 1) for $\omega = 1, \beta = 10$. We recap the stability of the fixed points and physical meaning for our problem in Table 1.

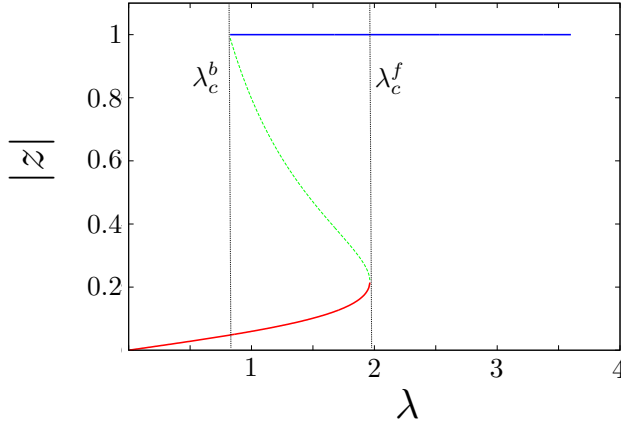


Figure 1: Dependence of the order parameter $|z|$ on the coupling λ . We show the critical forward and backward couplings for $\omega = 1, \beta = 10$. The red line shows the fixed point z_{a2} corresponding to the incoherent state. The green dashed line shows the fixed point with z_{a1} corresponding to the separatrix between coherent and incoherent states. Finally, the blue line shows the fixed points $z_{s1,2}$ with $|z_s| = 1$, which correspond to the coherent state.

Table 1: Fixed points of the order parameters with their stability and meaning.

Fixed Point	Stability	Existence Region	Physical Meaning
z_{s1}	sink	$\lambda > \lambda_c^b$	Coherent State
z_{s2}	source	$\lambda > \lambda_c^b$	none
z_{a1}	saddle	$\lambda_c^b > \lambda > \lambda_c^f$	separatrix
z_{a2}	center	$\lambda > \lambda_c^f$	Incoherent State

4 Numerics

Although the non-linear equation (7) for the order parameter is obtained in the thermodynamical limit, our numerical experiments reveal that finite size effects are negligible. Our predictions are in excellent agreement with the numerical experiments. We discuss this situation in some detail.

We have numerically simulated the model (1) using a fourth order Runge-Kutta integrator. We have focused on the forward transition. The experiments are performed as follows: For a fixed value of N and β , we start the simulations with $\lambda = 0$ and uniformly distributed initial conditions, then we integrate the model up to a time T . Then we increase the value of the coupling λ by a small amount and use the final step of the previous simulation as initial conditions. This procedure is known as following the attractor. Then for each step of this procedure we compute the order parameter $|z|$ as described in (4). Since we are computing the order parameter corresponding to the

incoherent state, we check our numerics against the thermodynamic limit described by z_{a2} . Our numerics shows that the agreement is excellent, see Fig. 2.

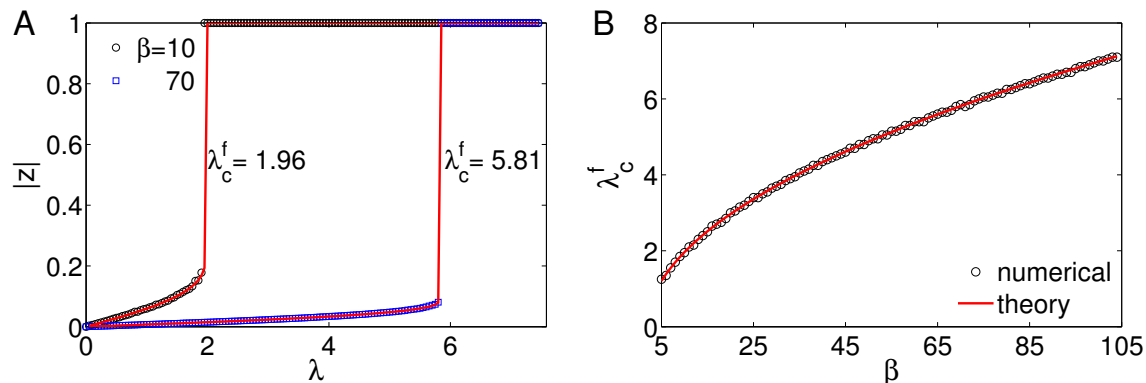


Figure 2: Numerical simulations of the forward transition for $N = 10000$. (A) Order parameter $|z|$ versus the coupling strength λ obtained numerically for $\beta = 10$ and $\beta = 70$. The full lines are the thermodynamical predictions z_{a2} . (B) The critical forward coupling λ_c^f versus the β . The numerical values are shown as open circles, while the (red) thick line is the theoretical prediction.

5 Conclusions

We have analyzed explosive synchronization for star graphs. We demonstrated that in the limit of infinitely many leave nodes the order parameter is governed by a nonlinear equation, which we were fully able to analyze. We showed the transitions towards and out of coherence are discontinuous. Moreover, we revealed the mechanism of discontinuity, namely, bifurcations of the order parameter create and annihilate fixed points forcing the loss of incoherence states (likewise the incoherent state).

In our model the parameter β controls the positive correlation between structure and dynamics. Our analysis shows that any positive correlation $\beta > 1$ leads to discontinuous transitions. Although, our macroscopic equations for the order parameters are particular to the star graphs, these graphs can be used as motifs to more intricate structures such as scale-free networks, see the discussion in Ref. [15]. Therefore, our results also shed light into the transitions in complex networks where the star motif is dominant.

Acknowledgments: This work was partially supported by DFG/FAPESP grant IRTG 1740/TRP 2011/50151-0. YZ was supported by NNSFC (Grant Nos. 11305062, 11135001, 81471651) (YZ) and TP by the Marie Curie IIF Fellowship (Project 303180).

References

- [1] A. Barrat, M. Barthelemy, A. Vespignani, *Dynamical Processes on Complex Networks*, Cambridge University Press (2008).
- [2] Nishikawa T., Motter A.E., Lai Y.-C. and Hoppensteadt F.C., Phys. Rev. Lett. **91** (2003) 014101; Motter A.E., Zhou C., and Kurths J., Phys. Rev. E **71**, 016116 (2005).
- [3] D.-S. Lee, Phys. Rev. E **72**, 026208 (2005).
- [4] T. Pereira, Physical Review E **82** (3), 036201 (2010).
- [5] J. Gomez-Gardenes, S. Gomez, A. Arenas, and Y. Moreno, Phys. Rev. Lett. **106**, 128701 (2011).
- [6] I. Leyva, R. Sevilla-Escoboza, J. M. Buldú, I. Sendinã Nadal, J. Gomez-Gardenes, A. Arenas, Y. Moreno, S. Gomez, R.Jaimes-Reategui, and S.Boccaletti, Phys. Rev. Lett. **108**, 168702 (2012).
- [7] T. K. D. Peron and F. A. Rodrigues, Phys. Rev. E **86**, 016102 (2012).
- [8] P. Ji, T. K. D. Peron, P. J. Menck, F. A. Rodrigues, J. Kurths, Phys. Rev. Lett. **110**, 218701 (2013).
- [9] P. S. Skardal, J. Sun, D. Taylor, and J. G. Restrepo, EPL (Europhysics Letters) **101**, 20001 (2013).
- [10] P. Li, K. Zhang, X. Xu, J. Zhang, and M. Small, Phys. Rev. E **87**, 042803 (2013).
- [11] W. Liu, Y. Wu, J. Xiao, and M. Zhan, EPL (Europhysics Letters) **101**, 38002 (2013).
- [12] I. Leyva, A. Navas, I. Sendinã Nadal, J. A. Almendral, J. M. Buldú, M. Zanin, D. Papo, and S. Boccaletti, Sci. Rep. **3**, 1281 (2013).
- [13] B. C. Coutinho, A. V. Goltsev, S. N. Dorogovtsev, and J. F. F. Mendes, Phys. Rev. E **87**, 032106 (2013).
- [14] T. K. D. Peron and F. A. Rodrigues, Phys. Rev. E **86**, 056108 (2012).
- [15] Y. Zou, T. Pereira, M. Small, Z. Liu, J. Kurths, Phys. Rev. Lett. **112**, 114102 (2014).
- [16] T. Pereira, D. Eroglu, G. B. Bagci, U. Tirnakli, and H. J. Jensen, Phys. Rev. Lett. **110**, 234103 (2013).
- [17] S. Watanabe and S. H. Strogatz, Phys. Rev. Lett. **70**, 2391 (1993).
- [18] S. Watanabe and S. H. Strogatz, Physica D **74**, 197 (1994).

[19] A. Pikovsky and M. Rosenblum, *Physica D* 240, 872 (2011).

[20] V. Vlasov, A. Pikovsky, E. E. N. Macau, unpublished (2014).